

# Understanding Current Background Noise Characteristics: Frequency and Time Domain Measurements of Noise on Multiple Locations

Alexandros Palaios<sup>(✉)</sup>, Vanya M. Miteva, Janne Riihijärvi,  
and Petri Mähönen

Institute for Networked Systems, RWTH Aachen University, Aachen, Germany  
[apa@inets.rwth-aachen.de](mailto:apa@inets.rwth-aachen.de)

**Abstract.** One of the important factors for the successful deployment of cognitive radio networks is keeping interference levels to minimum to primary users. The noise is usually expected to be thermal noise and non-interesting component on understanding a complex interplay between primary and secondary systems. Moreover, although usually it is assumed that excess interference is generated by secondary users it is worth of remembering that also primary systems generate harmonics and intermodulation components that can harm other primary systems. In this paper we report results from the measurement campaign that aims to find out how much there is excess noise over thermal noise floor. The observed noise levels cast questions on the widely used assumptions that we need to consider only AWGN thermal noise. We conclude the paper showing that the observed excess noise levels can have an effect on the capacity of the primary and secondary systems.

**Keywords:** Background noise characteristics · Frequency and time domain measurements · Noise on multiple locations · Interference levels

## 1 Introduction

There is a considerable body of work in the direction of how to minimize interference towards primary systems. Surprisingly though the hidden assumption is that the primary systems experience only thermal noise and any extra interference is caused by the secondary systems. However, transceiver chains are not built from ideally linear components and sharp filters. Thus many byproducts are still created and there is an open question how much primary systems themselves emit noise like components. This is important for both secondary and other primary access networks since emitted noise byproducts effectively raise the noise floor and cause reduced capacity. Moreover, the number of the wireless systems have tremendously increased, but the existing noise measurement literature is over 30 years old [1,2].

It is not only that wireless networks proliferated in the 1990s but also there has been shift from large cells supporting wireless telephony to small cells data

networks. Moreover, the number of services, networks and users has increased considerably the last twenty years [3].

The current literature on noise levels is very limited and is focusing either on studying time dynamics of very narrow frequency bands and thus but failing to capture how noise can be prevalent in wide bandwidths [4]. At the same time the pulse characteristics seem to be very dependent on devices emitting [5]. Finally, the available literature is focusing exclusively on specific transceiver technologies and modulation schemes [6]. All this limits the general understanding on observable noise levels.

We have recently finalized the first measurement campaign studying noise with wideband measurements (450 MHz to 3000 MHz). We have measured both indoor and outdoor environments trying to highlight the existence of noise on different representative localities such as city center, indoor office environments, transmission towers, industrial locations, power transmission lines and streets.

The rest of this paper is structured as follows. In Sect. 2 we describe our hardware configuration and the locations we studied. In Sect. 3 we present and discuss about the fundamental methodological problems on capturing noise levels, while not assuming cooperation from license owners. In Sect. 4 the exploratory data analysis is presented and in Sect. 6 we show how the observed noise levels can influence typical assumption made in link and network analysis. Finally, in Sect. 7 we present in details a specific example how noise can reduce the assumed capacity levels of systems. We conclude in Sect. 7.

## 2 Hardware Configuration and Locations Studied

We start by describing in details the studied locations and the hardware components used.

### 2.1 Locations Studied

For understanding the variability of noise sources and the shape of radio environment one has to do measurements with high spectral and time resolution. We have focused on large band spanning from 450 MHz to 3000 MHz and for the time domain we capture time dynamics on the order of milliseconds. Finally, it is also important to understand the variability in space. One assumes that noise changes over different localities and in this paper we report results from nine different locations. This selection is a subset from our larger planned measurement campaign. The locations captured in this study are summarized below

1. Office area: At this location both indoor (office rooms) and outdoor measurements were conducted.
  - (a) For the indoor measurements three different types of environments were chosen:
    - Empty office, with no electrical equipment inside it.
    - Working office, with a large number of office equipment devices (such as computers, phones and fluorescent lamps).

- Server room, where a large number of computational servers and electric cooling systems are working constantly.
- (b) Office district: The measurement setup was located next to a street with low to average amount of vehicle traffic. The location itself comprises mainly R&D companies and university buildings.
2. Street level at a business area: A crossroad with a low traffic intensity, located nearby the office district.
  3. TV tower: The measurement location is in the suburbs of the city, very close to the main radio and DVB-T tower of Aachen, which makes it a very good choice for examining the possible transmitted byproducts and out-of-band emissions in the DVB-T bands.
  4. City center: A measurement spot located in the part of the city, next to a busy road with high vehicle traffic.
  5. Power transmission lines: The location is right outside of the city, very close to a large number of high voltage transmission power lines. The measurement setup was positioned at around 50–70 meters from the main power lines.
  6. Factory: The measurements were conducted in a factory. During the measurement different high technology lasers were used for cutting, bending, sawing, and welding.

## 2.2 The Measurement Platform

The most important hardware component used is the high end spectrum analyzer (SA); the Agilent/Keysight E4440A. The device was selected due to its high sensitivity levels. The device achieves sensitivities below -125 dBm per 10 kHz for all the covered frequency spans. The tradeoff here is the power consumption. As we describe below we had to pay special attention for supporting portable measurements with such a heavy device. For supporting the operation of the SA as well as deploying our measurement setup on different locations we built a mobile measurement platform as depicted in Fig. 1 that contains three compartments. At the bottom there is a large car battery compartment that operates the spectrum analyzer when AC power is not available (a power converter was used to convert the DC power from the battery to AC). At the middle there is the SA compartment and above it there is the laptop compartment. The laptop controls the SA and stores the measurement data. The spectrum analyzer was calibrated by plugging in a  $50\Omega$  terminator at the RF input frontend. The last component of our setup is the high-end antenna (Schwarzbeck SBA 9113) that features very high degree of omnidirectionality. In some of the locations we had to turn off the preamplifier to protect the device from overloading. We specify later, in which locations preamplifier was turned off, leading to slightly lower sensitivity.

For the frequency type of measurements SA operated in sweep mode. Since an increased frequency resolution was important for spotting very narrowband signals (i.e. typically byproducts of a transmitter chain before the upconversion stage) and avoiding compression of those with large bandwidths, we selected to use a very narrow resolution bandwidth (RBW) of 10 kHz. The achieved time resolution between the different sweeps were on the order of tenths of seconds.



**Fig. 1.** The measurement Platform, a.k.a “Blue Box”. (Colour figure online)

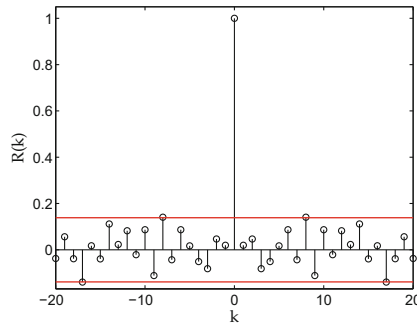


**Fig. 2.** Autocorrelation function of uncorrelated time series.

The 200 sweeps for the span of 450 MHz–3000 MHz last around 5 h and 30 min. The time domain measurements were conducted in zero span mode. During that time, the spectrum analyzer locks in to a fixed frequency with a given RBW at a fixed frequency and acquires the measurements faster than few microseconds. Both methods are useful but in this paper we focus mostly on frequency domain results. The frequency domain analysis has a priority as it provides us a baseline information on the seriousness of extra noise components in different frequency bands.

### 3 Tools for Noise Analysis

#### 3.1 Noise Definition

We start by explaining how we define noise in our measurements. We conducted power measurements, covering wide frequency bands, a large part of which are licensed and already used for transmission. Therefore, the existence of power

levels above the noise floor of the device can originate either from licensed transmitters or noisy byproducts. This means that methodologically one can not be sure if a reception is a noise byproduct or a weak licensed transmission. This is the reason we first look at the bands that are unlicensed or are used by weak licensed transmitters. We start by studying frequency bands that are unlicensed and no transmissions are allowed.

In Germany the Radio Astronomy band (1400 MHz to 1427 MHz) is a good example to monitor. Moreover, we included the cellular Guard Bands (Duplex Gap), such as the GSM, LTE and UMTS ones, as these should also be free from any intentional transmissions. For simplicity we call these bands as GSM 900, LTE 800 and UMTS but emphasize here that we are referring to their Guard Bands. Finally we observed also some licensed bands, most notably DVB-T digital-TV frequencies. In the commercial bands licenses are typically given with a specific spectrum mask (for the DVB-T system that is 8 MHz in Europe). In such a case observing very narrow band signals kHz is probably a noisy byproduct that should be considered as noise and not as part of licensed transmission.

### 3.2 Analysis Tools

Here we will present briefly the tools we used for processing our data and acquiring the characteristics of noise sources.

The autocorrelation analysis can be used to analyze whether subsequent values of time series are independent from each other. The normalized autocorrelation function (ACF)  $R$  for discrete time series  $X_T$  can be expressed as

$$R(k) = \frac{E[(X_T - \mu)(X_{T+k} - \mu)]}{\sigma^2}, \quad (1)$$

where the term in the numerator is the autocovariance and  $\sigma^2$  is the variance. For perfect white noise the ACF is a Dirac pulse. The confidence interval (CI) of a 95 % significance level is equal to

$$\text{CI} = [\mu - 1.96\sigma/\sqrt{n}; \mu + 1.96\sigma/\sqrt{n}], \quad (2)$$

where  $n$  is the number of samples. For uniformly distributed white noise ( $\mu = 0$  and  $\sigma = 1$ ) and  $n = 200$  the confidence interval becomes  $\text{CI} = [-0.1386 ; 0.1386]$ . Figure 1 shows an example of the ACF of uncorrelated time series with  $n = 200$ , including the corresponding confidence interval.

The Shapiro-Wilk (SW) test can be used to show divergence of a data distribution from the Gaussian one. It is defined as

$$W = \frac{\sum_{i=1}^n (a_i z_i)^2}{\sum_{i=1}^n (z_i - \bar{z})^2}, \quad (3)$$

where  $z_i$  is the  $i$ -th order statistic from an ordered random sample  $z_1 < z_2 < \dots < z_k$  and  $\bar{z}$  is the sample mean. The coefficients  $a_i$  are determined as

$$a_i = (a_1, a_2, \dots, a_k) = \frac{m^T V^{-1}}{\sqrt{m^T V^{-1} V^{-1} m}}, \tag{4}$$

where  $m = (m_1, m_2, \dots, m_k)^T$  is the vector of expected values of standard normal order statistics and  $V$  is the corresponding covariance matrix of those statistics. The value of the statistic  $W$  lies between zero and one, with a value of one indicating that the data has normal distribution.

In order to examine how the radio noise may affect deployed wireless networks we will have a look at channel capacity and how increased levels of radio noise could deteriorate it. As per Shannon-Hartley theorem the capacity of a certain channel can be calculated by

$$C = B \log_2(1 + S/N), \tag{5}$$

where  $B$  is the bandwidth of the channel in Hz,  $S$  is the average received signal power over the bandwidth in Watts and  $N$  is the average noise over the bandwidth also in Watts.

Firstly, we have to calculate a reference capacity for the particular technology, which we can compare with the measurements from the actual environment. The reference sensitivity needs to be set to the typical level a receiver has. For example, in the case of GSM the reference sensitivity level varies from -104 dBm to -87 dBm per 200 kHz of bandwidth for the different types of receivers [7]. The reference noise level is equal to:

$$N_{\text{ref}} = -174 + 10 \log_{10}(B) + NF \text{ dBm Hz} \tag{6}$$

where  $NF$  is the noise figure of the receiver.

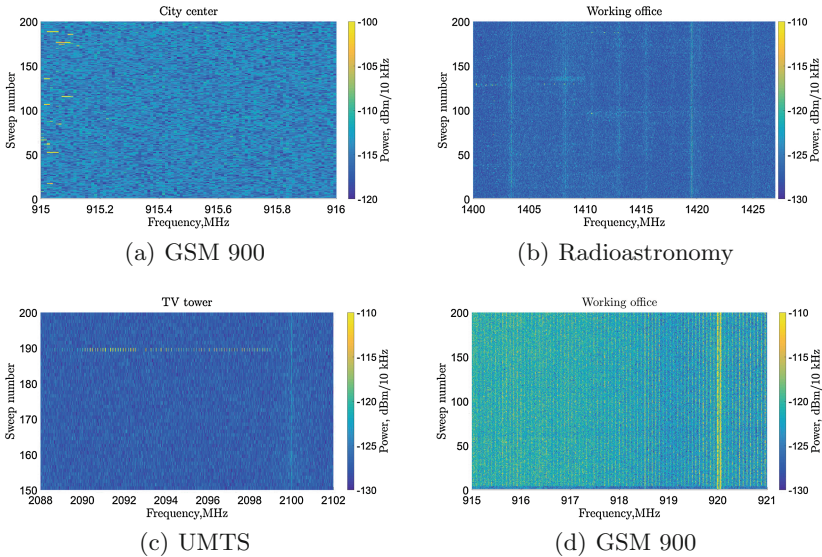


**Fig. 3.** Spectrograms of received power for different bands.

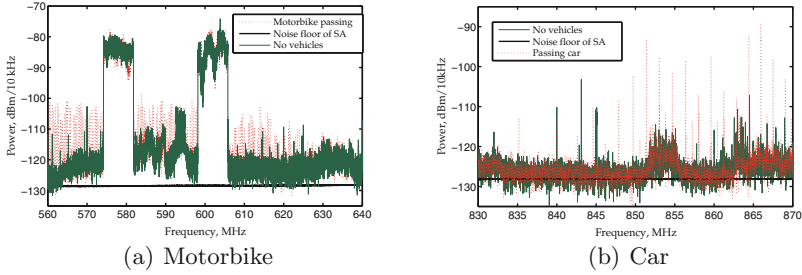


Fig. 4. Shapiro-Wilk time-frequency plots. (Color figure online)

### 4 Exploratory Data Analysis

We start by studying the noise characteristics of our measurements. We consider a typical outdoor scenario at the street level of the Business Area close to a road intersection. We study at part of the DVB-T and LTE bands to understand how vehicle traffic can affect the overall noise contribution. The measurement setup was located right next to the stop sign at the crossroad with the antenna at around 5 m distance from the passing vehicles. We measured the frequency range before there were any cars present and after different vehicles passed by our equipment.

Figure 4(a) depicts the results from the measurement when a motorbike passed by. It can be seen from the figure that a large number of byproducts appear with power levels of up to  $-100$  dBm/10 kHz. Figure 4(b) shows a second example of emitted byproducts when a car drove by our setup. One can see from the Figure that there are a large number of byproducts with levels of up to  $-90$  dBm/10 kHz, the majority of which is concentrated to a frequency band from 850 MHz to 870 MHz.

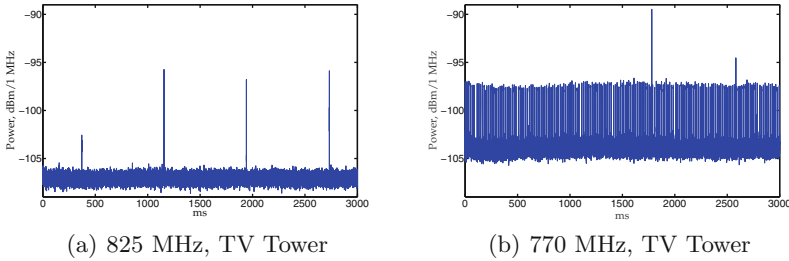


Fig. 5. Parts of the DVB-T band when different vehicles are passing by the measurement setup. (Color figure online)

We continue by analyzing the Radioastronomy and LTE 800 bands (that should be free of all man-made transmissions). The results for different location

**Table 1.** Mean power level and standard deviation for radioastronomy and LTE 800 guard band relative to the noise floor of the analyzer.

Location	Radioastronomy band		LTE800 Duplex Gap	
	rel. mean, dB	rel. $\sigma$ , dB	rel. mean, dB	rel. $\sigma$ , dB
<u>Amplifier On:</u>				
Empty Office	0	+0.0005	+0.078	+0.0034
Server room	+2.695	-0.0001	+7.282	+0.0276
Working Office	+1.205	+0.0635	+6.700	+0.3012
TV tower	+0.496	+0.0133	+0.047	+0.0249
<u>Amplifier Off:</u>				
City center	+0.328	-0.0013	+0.166	+0.0023
Office district	+0.307	-0.0009	+0.310	-0.0040
Transmission lines	0	-0.0029	+0.402	+0.0480
Working factory	+0.293	-0.0011	+0.240	+0.0038
Device Noise	mean, dBm	$\sigma$ , dB	mean, dBm	$\sigma$ , dB
Amplifier On	-127.299	1.7931	-128.184	1.7942
Amplifier Off	-114.590	1.7667	-114.255	1.7604

are shown in Table 1. We calculated the mean of the received power for the whole band. Regardless of the amplifier being off in some of the locations, a constant positive value was captured. One should note that indoor offices seem to have clearly persistent and strong excess noise levels. The reader should note that these results are aggregated statistics and smooth out details. Hence, they should be only used as a first step on finding the most noisy interesting bands to study in details.

## 5 Noise Variability

We continue by studying noise look like inside the different bands. In Fig. 3(a) the duplex gap of the GSM 900 band at the city center is depicted. The overall noise levels are slightly higher than in the other studied environments but the noise gets visible at the beginning of the band, at around 915 MHz that is concentrated around several frequency bins. It is also interesting that there is some time variation (sparks) and observed RX-power goes up to -100 dBm. Most likely, since this noise is located at the beginning of the band it might be an adjacent band transmission leaking outside the permitted frequency mask. One more representative example is shown in Fig. 3(b), for the Radioastronomy band observed in the working office environment. This is different for, Fig. 3(c), where the UMTS guard band in the working office is depicted. In the Fig. 3(c) there is only one constant time noisy byproduct at 2100 MHz and a very wide band one that is time dependent and lasts only for the duration of the sweep

(around 3s). Finally, we consider the GSM 900 guard band. The results are shown in Fig. 3(d), where the noise seems to be existing in the whole band with different spectral characteristics. Power levels vary also considerably with the strongest one being -110 dBm at 920 MHz. Such high noise levels with such idle spectrum coverage show that the specific working environment either has lots of electronic devices or some defective component is causing this behavior.

It is clear from the presented examples that noise varies a lot in frequency and time domain. As expected we have found that the noise is highly location dependent. The spatial persistence of noise components vary from few tens of meters to up to more than hundreds of meters. The aggregated statistics can make whole bands to look less noisier than what they in reality are.

We will provide one more example to highlight the very rich nature of noisy byproducts giving an example of the time dynamics. In Fig. 6 we show noise byproducts that the measurements captured nearby TV-transmission tower. The measurements were done in zero span mode at two different frequencies, namely in the 825 MHz and 770 MHz for the TV Tower environment. In Fig. 6(a), the captured signal consists interference (noise) bursts that are somehow interleaved around 800 ms or so. In Fig. 6(b) 770 MHz band is shown. The time dynamics of this “noise channel” is much richer and the signal is composed from bursts that repeat every few ms.

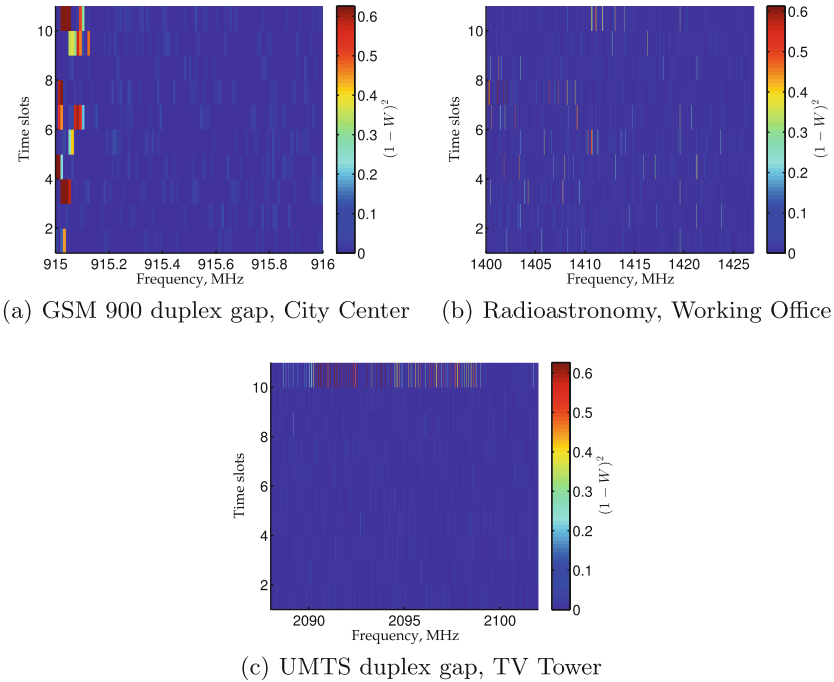


**Fig. 6.** Results from zero span measurements showing the detailed time domain structure of the noise.

## 6 Gaussianity Assumption

In this section we revisit AWGN channel assumptions [8–10]. Here, we would focus the Gaussianity characteristics of the AWGN channel and have a look at the time domain measurements to see if they resemble a Gaussian distribution. Finally, we study the time independency between samples that are also part of the AWGN channel.

For the Gaussianity we conducted the Shapiro-Wilk test (per frequency bin). That allows us to compare our captured data against the normal distribution. For this analysis we had to collect together multiple time domain measurements to calculate the Shapiro-Wilk statistic and thus 10 Shapiro-Wilk statistic time slots are given. Our first example is shown in Fig. 4(a) for the GSM 900 band in the City Center. The noise components around the 915 MHz that were described in the previous section are clearly seen as strong deviations from the Gaussianity assumption. We continue with Fig. 4(b) showing the Shapiro-Wilk statistics result for the Radioastronomy Band in the working office environment. The deviations from the Gaussian distribution are now well spread within the band and the problem is not just concentrated in few frequency bins as before. Finally in Fig. 4(c) we show results for the UMTS band where a strong deviation is captured that only lasted for some time before it disappeared. It is interesting though how widely the noise is spread within the band covering more than 12 MHz.

We continue by providing two more examples for the Radioastronomy and the UMTS duplex gap. In Fig. 7(a) the Radioastronomy band for the working office area is depicted. The corresponding spectrogram was already presented in Fig. 4(b) and the Shapiro-Wilk statistics do a good job capturing what we have described above. The deviations are spread all over the frequency band. In Fig. 7(b) the UMTS duplex gap for the TV tower location is shown. The deviations are not as widespread as before and tend to be concentrated at the beginning of the band and even more so at the end of the gap.

We finalize this section by analyzing also at the time independency assumption of subsequent samples. We calculated the autocorrelation for the measurement samples and the results are presented in Fig. 8. It is clear that for most of the captured frequency bins the autocorrelation gives a value which shows that

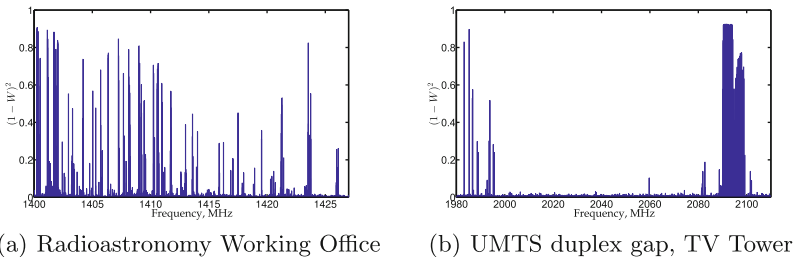


**Fig. 7.** Deviation from gaussianity assumption. Shapiro-Wilk tests.

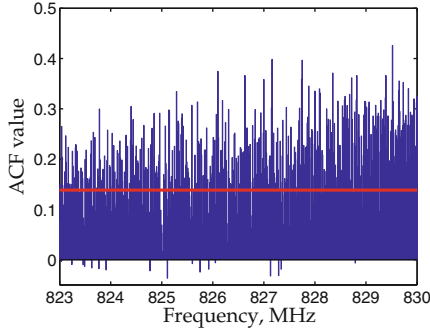


**Fig. 8.** Deviations from AWGN in the LTE Band in the working office. (Colour figure online)

the samples are not independent. The red line shows the limit for values to be considered independent and most of the values are larger than this threshold. Similar examples have been also found in other bands. From this set of measurements results it is clear that this large variability (frequency, time and locations) makes modeling of the excess noise rather difficult if not impossible.

## 7 Capacity Reduction from Increased Noise Levels

In this section we show how increased noise floor can impact the capacity of a radio systems. Digital receiver technology has progressed considerably on decoding and we are now able to exploit very weak signals. The sensitivity of receivers is superior to what they were 20 years ago. Thus, the increased noise levels have more impact on our system performance as we tend to operate in a low SNR regime, especially on the cell edges of mobile systems. We present first an example that is technology independent in the sense that we do not apply specific modulation and demodulation schemes. We employ the normalized capacity to calculate the lost capacity with excess noise. More specifically we evaluate the relative degradation of the Shannon spectral efficiency  $\log(1 + S/N)$  for a signal power  $S$  and noise level  $N$  for different values of the input parameters derived from the measurements. We calculate the reference capacity  $C_{\text{ref}}$  for each band assuming first only the thermal noise floor. We then repeat the calculation by adding the man-made interference to show how access noise components can have a similar effect as co-channel interference.

Figures 9(a) and (b) show that there is almost no reduction in the capacity for the empty office and the TV tower locations. However, for the rest of the locations the results at cell edge conditions can cause high capacity loss of up to 65 % and substantial reductions of up to 20 % even in rather high primary system power signal conditions, i.e., -80 dBm. The server room and the working office experience the highest MNP (Mean Noise Power) for the LTE800 and GSM900 duplex gaps compared to the other two locations. It is interesting to observe that the highest noise levels (that have some strong time domain constant type

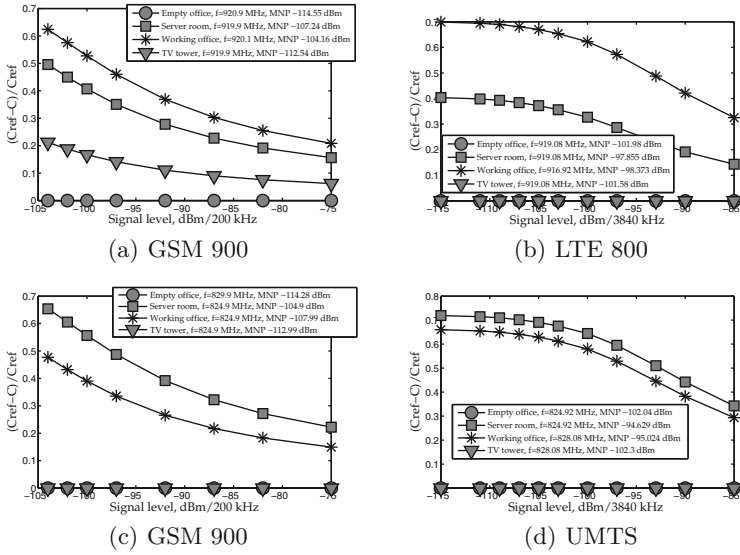


Fig. 9. Capacity reduction with the effect of measured noise.

of behavior) were spotted in the indoor environments. The reader should note that our measurements in the frequency domain were more prone in capturing long-time noise sources.

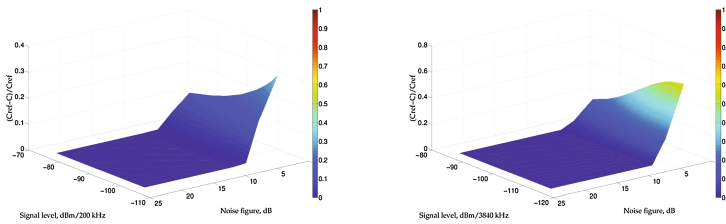
We continue estimating a possible capacity reduction for the LTE800 and the GSM900 technologies using measured values duplex gaps. In Figs. 9(c) and (d) we can see that the capacity reduction is a bit higher than in the GSM case. This is expected since the reference sensitivity for UMTS receivers is lower than the one for GSM. Situation is also similar for the empty office and the TV tower environments as before, although this does not necessarily mean that these locations are in total less noisy than others.

For the above results, we used a constant noise figure of 10 dB for the calculations of the capacity. Next, we give more examples that are based on today’s specific receivers noise figures. In the Table 2 we summarize typical values for several different technologies that were used in our calculations. We produce 3-D plots that allows the interested reader to see exactly how noise can affect different type of receivers.

Figure 10(a) presents the results when the capacity is calculated with respect to the GSM technology receiver sensitivities. The capacity reduction in the empty office has a constant behavior, i.e., equals zero, down to noise figure of 7 dB, after which it starts gradually increasing. In such case the UMTS and LTE base stations, which generally have low noise figures as seen from Table 2, might experience problems. However, for receivers using Bluetooth and ZigBee technology, which have higher noise figures, as expected will not be affected by these noise levels.

**Table 2.** Typical noise figure for various technologies.

Technology	Noise figure, dB
GSM900	7
UMTS:	
Base station	2
User equipment	7
LTE:	
Base station	5
User equipment	9
802.11 (WLAN)	10
Bluetooth	23
ZigBee	20



(a) LTE duplex gap, Empty Office, GSM technology, (b) LTE duplex gap, TV tower, UMTS technology

**Fig. 10.** Examples of the theoretical capacity reduction.

Finally, Figs. 10(a) and (b) also allow us to compare how the same noise could affect different technologies. We see from the Figures that for the same locations and frequencies the capacity reduction for the GSM case is lower compared to the UMTS one, which is due to the more strict requirements on the reference sensitivity of the receiver in UMTS.

## 8 Conclusions

In this paper we reported preliminary results from our high-resolution noise measurement campaign. We have shown that the noise has very different characteristics in different localities, both in frequency and time domains. Aggregated statistics at the same time can not represent exact noise levels since they heavily average out the noisy byproducts.

We were able to observe strong radio noise in all locations at different frequency bins and time scales, which shows that man-made noise level has significantly increased. It is at these levels that should be taken into account from contemporary designs of new-systems, and particularly be considered by dynamic

spectrum access community. We show strong deviations from the theoretical Gaussian model. Whiteness of the noise, time independency, and the Gaussian structure of noise were found to not hold for many different frequency and time bands on different localities. Finally we would like to stress that noise measurements are not just new spectrum measurements focusing on the low level signals, but are a distinct type of characterization of the radio environment with unique challenges.

**Acknowledgment.** The authors would like to thank RWTH Aachen University and the German Research Foundation (Deutsche Forschungsgemeinschaft, DFG) for providing financial support.

## References

1. Middleton, D.: Man-made noise in urban environments and transportation systems: models and measurements. *IEEE Trans. Veh. Technol.* **22**(4), 148–157 (1973)
2. Gemikonakli, O., Aghvami, A.: Impact of non-Gaussian noise on the performance of M-ary CPSK signalling transmitted through two-link nonlinear channels. *IEEE Proc. Commun. Speech Vis.* **136**(5), 328–332 (1989)
3. Bangerter, B., Talwar, S., Arefi, R., Stewart, K.: Networks and devices for the 5G era. *IEEE Commun. Mag.* **52**(2), 90–96 (2014)
4. Chandra, P.: Measurements of radio impulsive noise from various sources in an indoor environment at 900 MHz and 1800 MHz. In: *The 13th IEEE International Symposium on Personal, Indoor and Mobile Radio Communications*, pp. 639–643, vol. 2, September 2002
5. Shongwey, T., Vinck, A., Ferreira, H.: On impulse noise and its models. In: *18th IEEE International Symposium on Power Line Communications and its Applications*, pp. 12–17, March 2014
6. Unawong, S., Miyamoto, S., Morinaga, N.: Receiver design of CDMA system for impulsive radio noise environment. In: *International Symposium on Electromagnetic Compatibility Proceedings*, pp. 316–319, May 1997
7. ETSI TS 145 005 V12.5.0 Digital cellular telecommunications system (Phase 2+); Radio Transmission and Reception, ITU-R, Technical report, April 2015
8. Suraweera, H., Smith, P., Surobhi, N.: Exact outage probability of cooperative diversity with opportunistic spectrum access. In: *IEEE International Conference on Communications Workshops*, pp. 79–84, May 2008
9. Atapattu, S., Tellambura, C., Jiang, H.: Energy detection based cooperative spectrum sensing in cognitive radio networks. *IEEE Trans. Wirel. Commun.* **10**(4), 1232–1241 (2011)
10. Ubaidulla, P., Aissa, S.: Optimal relay selection and power allocation for cognitive two-way relaying networks. *IEEE Wirel. Commun. Lett.* **1**(3), 225–228 (2012)